Microwave Imaging of Three-Dimensional Conducting Objects Using the Newton Minimization Approach

Aslan Etminan[1,2] and Levent Gürel[1,2]

[1]*Electrical and Electronics Engineering Department, Bilkent University, TR-06800 Ankara, Turkey*
[2]*Computational Electromagnetics Research Center (BiLCEM), Bilkent University, TR-06800 Ankara, Turkey*
aslan@ee.bilkent.edu.tr

***Abstract*— In this work, we present a framework to detect the shape of unknown perfect electric conducting objects by using inverse scattering and microwave imaging. The initial-guess object, which evolves to achieve the target, is modeled by triangles such that vertices of the triangles are the unknowns of our problem.**

I. Introduction

Object detection is used in a wide range of applications, from detecting cancer tumors to finding buried objects [2],[3],[4]. The first aim of object detection is to find the location and shape of an unknown target. Various methods are applied to detect objects in different applications, and some of the most important challenges involve overcoming non-linearity and non-uniqueness of the solutions.

Inverse scattering is one of the most efficient ways to retrieve the shapes and locations of targets. By illuminating the objects with electromagnetic waves and collecting the scattered fields, we try to obtain the shape of unknown object. We begin with an initial guess of the unknown object. Then, by comparing the scattered far-field patterns of the initial-guess object and the real object, we evolve the initial-guess object and update it iteratively such that we gradually decrease the difference between the patterns. Finally, we achieve a match with the unknown object.

In this paper, we model the object by one of its parameters, such as the location of its surface nodes or by the conductivity, permittivity, and permeability of the discretized space that holds the object. Then, the model parameters are updated iteratively by minimizing the mismatch between the measured data of the target and the collected data from the modeled object. Location of the surface nodes is a good choice of parameter because we can decrease the number of unknowns, compared to volume modeling.

II. Cost Function

We need to define a criterion to determine the difference between the target object and the evolving object, the latter of which should ultimately match the target. A suitable criterion is the total mismatch of the measurements between the target and the evolving object. Residual vector is defined as the mismatches of measurements between the target and evolving object that can be shown as

$$\boldsymbol{e}(\boldsymbol{x}) = \begin{bmatrix} e_1(\boldsymbol{x}) \\ \vdots \\ e_M(\boldsymbol{x}) \end{bmatrix}, \tag{1}$$

where $e_j(\boldsymbol{x}) = S_j(\boldsymbol{x}) - m_j$ is the mismatch between the jth measured data from the evolving object $S_j(\boldsymbol{x})$ and the jth measured data from target m_j, and M is the number of measurements. $\boldsymbol{x}$ is the unknown vector, which in our case consists of the node coordinates.

We can define the summation of the magnitude of the measurement mismatches as the cost function, that is the above mentioned criterion. Hence, we define the cost function as

$$C(\boldsymbol{x}) = \sum_{i=1}^{M} ||e_i(\boldsymbol{x})||^2. \tag{2}$$

III. The Newton Minimization Approach

The goal in our minimization problem is to update the unknown vector such that the cost function decreases at each iteration. Thus, by using the Taylor-series expansion of the cost function, and considering the first three terms of this expansion, the quadratic form of the cost function will be obtained around the unknown vector $\boldsymbol{x}_k$ of the kth iteration [1]:

$$C(\boldsymbol{x}_k+\boldsymbol{p}_k) \approx C(\boldsymbol{x}_k)+\nabla C(\boldsymbol{x}_k)^T \cdot \boldsymbol{p}_k+\frac{1}{2}\boldsymbol{p}_k^T \cdot \nabla\nabla C(\boldsymbol{x}_k) \cdot \boldsymbol{p}_k, \tag{3}$$

where $\boldsymbol{p}_k$ is the step vector that will update the unknown vector in the kth iteration. To find the gradient vector $\boldsymbol{g}(\boldsymbol{x}_k) = \nabla C(\boldsymbol{x}_k)$ and the Hessian matrix $\overline{\boldsymbol{G}}(\boldsymbol{x}_k) = \nabla\nabla C(\boldsymbol{x_k})$, we expand the cost function in terms of the complex-valued residuals of the measurements. Thus, we can write the cost function as

$$C(\boldsymbol{x}_k) = \boldsymbol{e}^H(\boldsymbol{x}_k) \cdot \boldsymbol{e}(\boldsymbol{x}_k) = e_1^* e_1 + ... + e_M^* e_M, \tag{4}$$

where the superscript H signifies the complex conjugate and transpose of the vector. Using Eq. (4), the gradient vector can be written as

978-1-4799-1434-0/13/$31.00 ©2013 IEEE

$$\boldsymbol{g}(\boldsymbol{x}_k) = \nabla C(\boldsymbol{x}_k)$$

$$= \left[\begin{array}{ccccc} \dfrac{\partial C}{\partial x_1} & \cdots & \dfrac{\partial C}{\partial x_i} & \cdots & \dfrac{\partial C}{\partial x_N} \end{array} \right]^T$$

$$= \begin{bmatrix} 2\,\mathrm{Re}\left\{ \left(\frac{\partial}{\partial x_1} \boldsymbol{e}^H(\boldsymbol{x}) \right) \cdot \boldsymbol{e}(\boldsymbol{x}) \right\} \\ \vdots \\ 2\,\mathrm{Re}\left\{ \left(\frac{\partial}{\partial x_i} \boldsymbol{e}^H(\boldsymbol{x}) \right) \cdot \boldsymbol{e}(\boldsymbol{x}) \right\} \\ \vdots \\ 2\,\mathrm{Re}\left\{ \left(\frac{\partial}{\partial x_N} \boldsymbol{e}^H(\boldsymbol{x}) \right) \cdot \boldsymbol{e}(\boldsymbol{x}) \right\} \end{bmatrix}$$

$$= 2\,\mathrm{Re}\left\{ \overline{\boldsymbol{J}}^H(\boldsymbol{x}_k) \cdot \boldsymbol{e}(\boldsymbol{x}) \right\}, \tag{5}$$

where

$$\overline{\boldsymbol{J}}(\boldsymbol{x}) = \begin{bmatrix} \frac{\partial}{\partial x_1} e_1 & \cdots & \frac{\partial}{\partial x_N} e_1 \\ \vdots & \ddots & \vdots \\ \frac{\partial}{\partial x_1} e_M & \cdots & \frac{\partial}{\partial x_N} e_M \end{bmatrix} \tag{6}$$

is the Jacobian matrix of the residual vector. We use a numerical method to compute the elements of the Jacobian matrix, as explained in the next section. To obtain the Hessian matrix, we take the gradient of (5) to obtain

$$\overline{\boldsymbol{G}}(\boldsymbol{x}_k) = \nabla\nabla C(\boldsymbol{x}_k) = 2\,\mathrm{Re}\{\overline{\boldsymbol{J}}^H(\boldsymbol{x}) \cdot \overline{\boldsymbol{J}}(\boldsymbol{x}) + \overline{\boldsymbol{Q}}(\boldsymbol{x})\}, \tag{7}$$

where $\overline{\boldsymbol{Q}}(\boldsymbol{x}) = \sum_{m=1}^{M} e_m(\boldsymbol{x}) \overline{\boldsymbol{F}}_m^H$ and $\overline{\boldsymbol{F}}_m = \nabla\nabla e_m(\boldsymbol{x})$.

A. Optimization of the Cost Function

Methods that require the computation of the inverse of the Hessian matrix $\overline{\boldsymbol{G}}(\boldsymbol{x}_k)$ to optimize the cost function are not suitable when we have a large number of unknowns. As a result, we apply the steepest-descent method, which gives the step vector $\boldsymbol{p}_k$ in the opposite direction to the gradient vector of the cost function:

$$\boldsymbol{p}_k = -\gamma_k \nabla C(\boldsymbol{x}_k) = -\gamma_k \boldsymbol{g}_k. \tag{8}$$

By substituting Eq. (8) in Eq. (3), we obtain:

$$C(\boldsymbol{x}_k + \boldsymbol{p}_k) \approx C(\boldsymbol{x}_k) - \gamma_k |\boldsymbol{g}_k|^2 + \frac{1}{2} \gamma_k^2 \boldsymbol{g}_k^T \cdot \overline{\boldsymbol{G}}(\boldsymbol{x}_k) \cdot \boldsymbol{g}_k. \tag{9}$$

Since our goal is to decrease the cost function, we need to minimize the last two terms of the (9). Therefore, γ_k should be chosen as

$$\gamma_k = -\frac{|\boldsymbol{g}_k|^2}{\boldsymbol{g}_k^T \cdot \overline{\boldsymbol{G}}(\boldsymbol{x}_k) \cdot \boldsymbol{g}_k} \tag{10}$$

$$\Rightarrow \boldsymbol{p}_k = -\frac{|\boldsymbol{g}_k|^2}{\boldsymbol{g}_k^T \cdot \overline{\boldsymbol{G}}(\boldsymbol{x}_k) \cdot \boldsymbol{g}_k} \boldsymbol{g}_k. \tag{11}$$

B. Numerical Calculation of the Jacobian Matrix

To obtain the gradient vector $\boldsymbol{g}$ and the Hessian matrix $\overline{\boldsymbol{G}}$, the Jacobian matrix of the residual vector is required. We used a numerical method to calculate the Jacobian matrix. In this method, for each column of the Jacobian matrix, the corresponding unknown of that column is slightly perturbed, and then the change in each measurement is calculated. Finally, by using the first-order derivative approximation, each element of the column is calculated. In choosing the perturbation size, we should consider reasonable upper and lower limits. One of the parameters that can determine the upper limit of the perturbation size is the mesh size of the object. Clearly, perturbations that are larger than the mesh size will change the topology of the object. In addition, numerical calculation of the derivatives imposes an upper limit for the perturbation size. Obviously, large perturbation sizes lead to less accurate numerical results. On the other hand, the lower limit of choosing the perturbation size depends on the computational accuracy of the forward solver, which computes the scattered electric fields.

IV. Numerical Results

We reconstructed several conducting objects, such as spheres, ellipsoids, and star shapes. In all cases, three components of the node locations were assumed to be the unknowns. For brevity, only the results corresponding to the reconstruction of a star-shaped object are presented in this paper. We use 12 incident plane waves from 6 directions with theta and phi polarizations to illuminate the target, and 26 scattering directions per incidence in the reconstruction algorithm. The incident directions are the $\pm x$, $\pm y$, and $\pm z$ directions, and the scattering directions were uniformly distributed around the targets. The operating frequency was 10 GHz.

The initial-guess object was chosen to be a sphere of radius 10 mm centered at the origin. The radius of the star-shaped target changes between 11 mm and 15 mm, and the target is centered at the origin. As evident in Fig. 1, the evolving object approaches the general shape of the target in the first three iterations, and in the following iterations the object is completely reconstructed. The cost function at each iteration is shown in Fig. 2, where we can see a decrease in the cost function, especially in the first five iterations. In the 25th iteration, the cost function is decreased to 2.9% of its initial value (below the stopping condition of 3%); therefore, the program is stopped in this iteration.

The results show that we achieve a significant reduction in the cost function in the first few iterations, and thus the target object's general shape will be quickly obtained. However, in the following iterations, the speed of reduction of the cost function decreases. Thus, the convergence of the cost function to zero slows down.

V. Conclusions

In an effort to achieve the microwave imaging of three-dimensional conducting objects, we use the Newton minimization formulation to solve the inverse scattering problem.

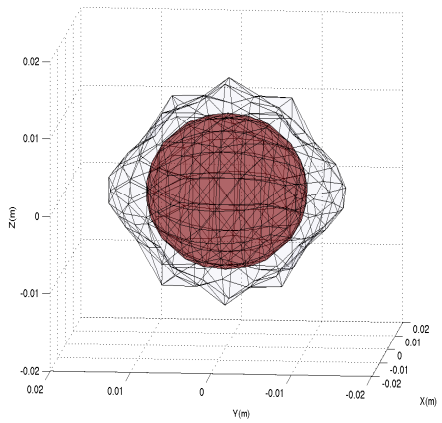

(a)

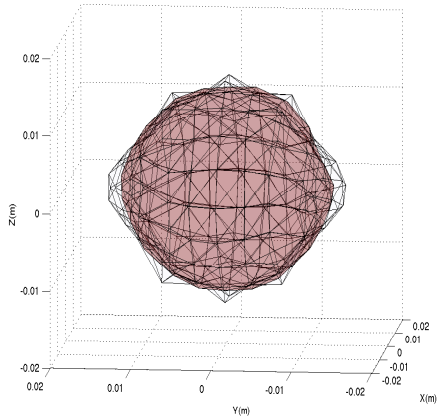

(b)

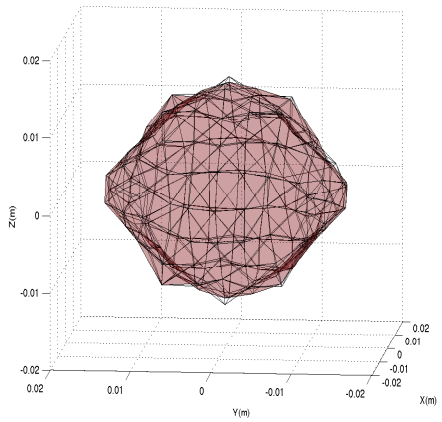

(c)

Fig. 1. Reconstruction of a star-shaped object at 10 GHz, where the transparent object is our target and the red object is the evolving object. (a) Initial guess, (b) after three iterations, and (c) after 20 iterations.

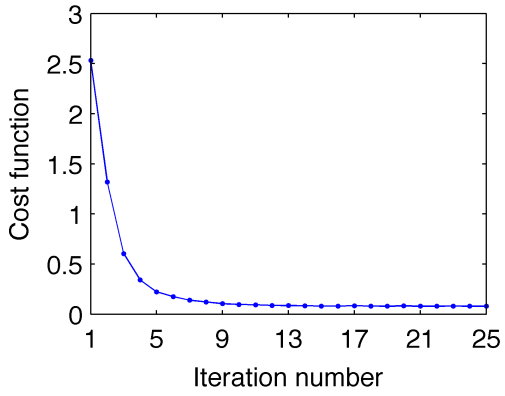

Fig. 2. Cost function for the reconstruction of a star-shaped object.

Following a rigorous formulation, we compute the Jacobian matrix by employing a fully numerical approach. To this end, derivatives of the cost function are obtained numerically. This requires the efficient solution of a large number of forward problems. We present results to demonstrate that the shape reconstruction of various conducting objects can be successfully accomplished.

ACKNOWLEDGMENT

This work was supported by the Scientific and Technical Research Council of Turkey (TUBITAK) under Research Grants 110E268 and 111E203, by Schlumberger-Doll Research (SDR), and by contracts from ASELSAN, Turkish Aerospace Industries (TAI), and the Undersecretariat for Defense Industries (SSM).

REFERENCES

[1] T. M. Habashy and A. Abubakar, "A general framework for constraint minimization for the inversion of electromagnetic measurements," *Prog. Electromagn. Res.*, vol. 46, pp. 265–312, 2004.

[2] A. Abubakar, T. M. Habashy, V. L. Druskin, L. Knizhnerman, and D. Alumbaugh, "A 2.5D forward and inverse modeling for interpreting low-frequency electromagnetic measurements," *Geophysics*, vol. 73, no. 4, pp. F165–F177, Aug. 2008.

[3] H. Zhou, T. Takenaka, J. Johnson, and T. Tanaka, "A breast imaging model using microwaves and a time domain three dimensional reconstruction method," *Prog. Electromagn. Res.*, vol. 93, pp. 57–70, 2009.

[4] I. Catapano, L. Crocco, and T. Isernia, "Improved sampling methods for shape reconstruction of 3-D buried targets," *IEEE Trans. Geosci. Remote Sens.*, vol. 46, no. 10, pp. 3265–3273, Oct. 2008.

[5] J. A. Sethian, *Level Set Methods and Fast Marching Methods*. Cambridge: Cambridge University Press, 1999.